Protein Science (1995), *4*:1844–1850. Cambridge University Press. Printed in the USA.

The role of aspartate-235 in the binding of cations to an artificial cavity at the radical site of cytochrome *c* peroxidase

MELISSA M. FITZGERALD, MICHELLE L. TRESTER, GERARD M. JENSEN, DUNCAN E. MCREE, AND DAVID B. GOODIN

Department of Molecular Biology, The Scripps Research Institute, La Jolla, California 92037

(RECEIVED April 17, 1995; ACCEPTED June 14, 1995)

Abstract

The activated state of cytochrome *c* peroxidase, compound ES, contains a cation radical on the Trp-191 side chain. We recently reported that replacing this tryptophan with glycine creates a buried cavity at the active site that contains ordered solvent and that will specifically bind substituted imidazoles in their protonated cationic forms (Fitzgerald MM, Churchill MJ, McRee DE, Goodin DB, 1994, *Biochemistry 33*:3807–3818). Proposals that a nearby carboxylate, Asp-235, and competing monovalent cations should modulate the affinity of the W191G cavity for ligand binding are addressed in this study. Competitive binding titrations of the imidazolium ion to W191G as a function of $[K^+]$ show that potassium competes weakly with the binding of imidazoles. The dissociation constant observed for potassium binding (18 mM) is more than 3,000-fold higher than that for 1,2-dimethylimidazole (5.5 μM) in the absence of competing cations. Significantly, the W191G–D235N double mutant shows no evidence for binding imidazoles in their cationic or neutral forms, even though the structure of the cavity remains largely unperturbed by replacement of the carboxylate. Refined crystallographic *B*-values of solvent positions indicate that the weakly bound potassium in W191G is significantly depopulated in the double mutant. These results demonstrate that the buried negative charge of Asp-235 is an essential feature of the cation binding determinant and indicate that this carboxylate plays a critical role in stabilizing the formation of the Trp-191 radical cation.

Keywords: cytochrome *c* peroxidase; engineered binding site; enzyme–substrate binding; protein cavities; protein engineering; tryptophan radical cation; X-ray crystallography

The mechanism by which cytochrome *c* peroxidase (CCP) produces and stabilizes the Trp-191 radical cation of its compound ES state is incompletely characterized. In compound ES, the heme is converted to an oxyferryl state, $Fe^{+4}=O$, and Trp-191 is oxidized to a cation free radical (Erman et al., 1989; Scholes et al., 1989; Sivaraja et al., 1989; Houseman et al., 1993; Huyett et al., 1995). A nearby carboxylate, Asp-235, makes a hydrogen bond with both the heme ligand, His-175, and with the indole NH of Trp-191 (Finzel et al., 1984). Asp-235 has been shown to control the properties of His-175 as a heme ligand, to influence the electrochemical properties of the heme, and to modulate the coupling between the heme and the Trp-191 radical (Dasgupta et al., 1989; Satterlee et al., 1990; Spiro et al., 1990; Vitello et al., 1992; Goodin & McRee, 1993; McRee et al., 1994). It is also reasonable that the buried charge of Asp-235 may significantly stabilize the formation of the Trp-191 cation radical by an electrostatic charge-pair interaction. Of the mutants of Asp-235 that have been described, only D235E, which retains a carboxylate side chain, has been shown to form a stable Trp-191 radical (Fishel et al., 1991; Goodin & McRee, 1993). However, because the tryptophan ring conformation is significantly altered in the D235N and D235A mutants (Wang et al., 1990; Goodin & McRee, 1993), the direct role of Asp-235 in the stabilization of the Trp-191 radical has not been clearly defined.

In a recent study (Fitzgerald et al., 1994), we exploited the ability of the enzyme to stabilize a cationic species at the Trp-191 radical site by introducing an artificial cation binding site

Reprint requests to: David B. Goodin, Department of Molecular Biology, MB8, The Scripps Research Institute, 10666 North Torrey Pines Rd., La Jolla, California 92037; e-mail: dbg@scripps.edu.

Abbreviations: CCP, cytochrome *c* peroxidase; APX, ascorbate peroxidase; CCP-(MKT) cytochrome *c* peroxidase produced by expression in *Escherichia coli* and containing Met-Lys-Thr at the N-terminus; compound ES, the H_2O_2 oxidized state of cytochrome *c* peroxidase; W191G, cytochrome *c* peroxidase mutant in which Trp-191 is replaced with Gly; D235N, mutant in which Asp-235 is replaced with Asn; W191G–D235N, double mutant in which Trp-191 is replaced with Gly and Asp-235 is replaced with Asn; MPD, 2-methyl-2,4-pentanediol; BTP, BIS-TRIS propane; DMI, 1,2-dimethylimidazole; DMI^+, 1,2-dimethylimidazolium ion; F_{DMI}, structure factor amplitude of W191G or W191G–D235N crystals soaked in 1,2-dimethylimidazole; F_{K^+}, structure factor amplitude of W191G or W191G–D235N crystals soaked in potassium phosphate.

into the enzyme. The Trp-191 to Gly mutation resulted in the formation of a well-defined and completely buried cavity on the proximal side of the heme, which contained ordered solvent molecules in place of Trp-191. By measuring the effects of probe molecules on the heme Soret absorption, we found that imidazole derivatives bind to W191G and obtained evidence from the effect of pH on binding that these compounds were bound as the positively charged imidazolium ions. Structural analysis of W191G crystals soaked in various imidazoles revealed electron density in the cavity, which was consistent with an interaction between the protonated imidazole nitrogen and Asp-235. We concluded that the cation determinant for imidazole binding appears to result significantly from the interaction between the probe molecule and the carboxylate of Asp-235, and that an analogous interaction may stabilize the developing positive charge on the Trp-191 radical in native CCP.

Subsequent to this report (Fitzgerald et al., 1994), the binding of cations to a W191G mutant of CCP was independently confirmed (Miller et al., 1994). Structural analysis of an independent W191G mutant (Miller et al., 1994) indicated that buffer cations such as Na^+, K^+, $Tris^+$, and NH_4^+ were found in the cavity at a position that differed somewhat from that observed by us for imidazole binding. These buffer cations were observed at a site equivalent to one of the five solvent electron density peaks originally observed in the ligand-free crystal structure of W191G (Fitzgerald et al., 1994), and it was suggested that this peak, which we had modeled as H_2O-400, was in fact a buffer cation. This site is similar to a consensus K^+ binding site formed at a Type III turn in which the backbone carbonyl oxygen atoms of residues 175 and 177 are ligands to the metal (Miller et al., 1994). These authors concluded from this structural evidence that, more generally, the cation binding site created by W191G is not near the carboxylate of Asp-235 or at the site of imidazolium binding, but is instead at the location of the observed potassium ion. This conclusion was based in part upon a statement that very weak binding by imidazoles competes poorly for the strongly bound buffer cations observed in their study. However, no data were presented or cited to support these claims in spite of the earlier results (Fitzgerald et al., 1994) in which six different imidazole derivatives were observed to displace the ordered solvent peaks in the W191G cavity with K_d values ranging from 30 μM to 3 mM. We note that, although the alkali metal and imidazolium binding sites are spatially distinct, they would be expected to be mutually exclusive. These data would appear to indicate that the overall specificity of this cavity for ligands is more complex than the issue of where the "cation binding site" is located. Thus, the mechanism and specificity by which the cavity at the Trp-191 radical site stabilizes the binding of species ranging from simple buffer ions to cationic heterocyclic compounds are in need of a more complete characterization.

In the present study, competitive binding experiments are used to show that imidazolium and its derivatives bind the W191G cavity with up to 3,000-fold higher affinity than does K^+. In addition, crystallographic characterizations of the W191G-D235N double mutant show that replacement of the negatively charged carboxylate has little structural effect on the cavity dimensions, yet abolishes all crystallographic and spectroscopic evidence of binding by cationic species. The carboxylate at residue 235 is therefore an essential feature of the cation-specific binding exhibited by the W191G cavity, irrespective of the type of cation. These measurements more clearly define the interactions that confer binding specificity on an artificial cavity and demonstrate the importance of charge stabilization in an engineered binding site.

Results

Competitive binding measurements show that monovalent cations such as K^+ compete poorly with the relatively strong binding by imidazoles within the cavity of W191G. Optical absorption titrations of W191G with imidazole were carried out over a range of K^+ concentrations in 100 mM BTP buffer, pH 6. BTP was chosen because it is too large to fit within the W191G cavity and thus the solution could be buffered independently of the concentration of competing cations. The results of a competitive binding experiment are presented in Figure 1 and show that the apparent dissociation constant for imidazole binding to W191G, K_{obs}, is a linear function of $[K^+]$. The previously reported dissociation constant of 0.70 mM in 100 mM potassium phosphate buffer at pH 6 ($[K^+] = 92$ mM) (Fitzgerald et al., 1994) is also included in Figure 1. This value is in excellent agreement with the trend in K_{obs} obtained in the present study as a function of $[K^+]$. The dissociation constant for K^+ binding to W191G, K_I, was determined to be 18 mM from the linear least-squares fit of the data to $K_{obs} = K_d + (K_d/K_I)[K^+]$. The dissociation constant for imidazolium binding in the absence of competing K^+, K_d, was determined to be 0.11 mM from the linear least-squares fit. In the previous study (Fitzgerald et al., 1994), we observed that DMI^+ binds to the W191G cavity with a significantly higher affinity than does imidazolium and concluded that this is due, in part, to a more efficient filling of the cavity dimensions. As with imidazole, we now find that the binding affinity of DMI^+ to W191G is similarly increased by exclusion of competing K^+ from the solution. In this case, the K_d for DMI^+ binding to W191G decreases from 27 μM in the presence of 92 mM K^+ (Fitzgerald et al., 1994) to 5.5 μM in 100 mM BTP, pH 6. Thus, imidazolium binds with 150-fold higher affinity, and DMI^+ binds with 3,300-fold higher affinity to the W191G cavity relative to potassium binding. These experimental data are in direct opposition to assertions made by Miller et al. (1994) that the imidazolium ion competes poorly with buffer cations in the cavity of W191G.

The W191G-D235N double mutant was constructed to directly test the hypothesis that the potentially charged Asp-235 contributes to the cation binding determinant of the cavity created by removal of Trp-191. Optical absorption titrations of W191G-D235N with imidazole under a number of buffer conditions from pH 5.8 to 8.0 showed only small perturbations in the Soret region. Furthermore, these changes were no different than the small, nonsaturating changes observed for control D235N protein samples (data not shown) and could thus not be attributed to binding equilibria involving the cavity. From these experiments, we estimate a lower limit for K_d of these compounds to be about 50 mM. The absence of observed binding over a range in pH that spans the pK_a for imidazole in solution ($pK_a = 7.3$) (Katritzky & Rees, 1984) indicates that W191G-D235N does not bind imidazole in either the charged or neutral states. Likewise, no evidence for DMI or DMI^+ binding to W191G-D235N was observed by similar optical titrations. These observations are in contrast to the readily measurable 1-2% intensification of the Soret band resulting from imidazolium bind-

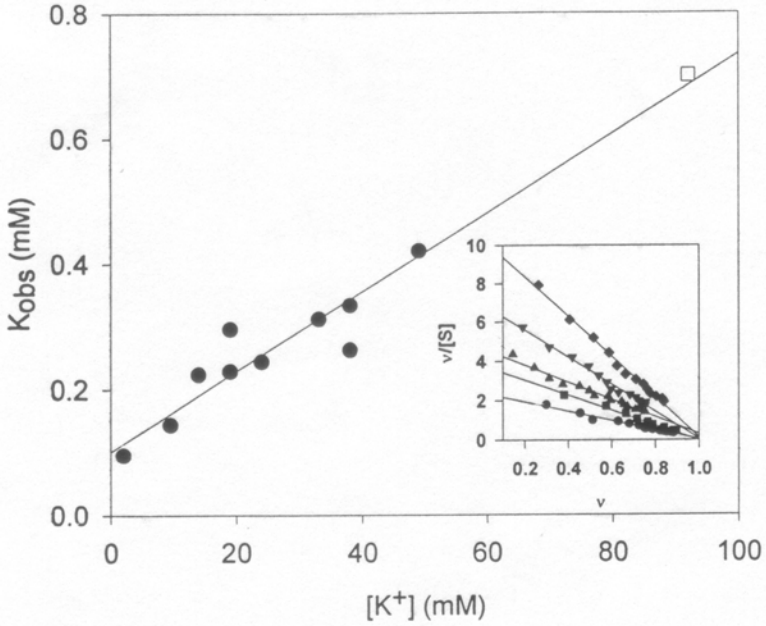

Fig. 1. Effect of $[K^+]$ on the observed dissociation constant (K_{obs}) for the binding of imidazole to W191G. K_{obs} for imidazole was determined from Scatchard plots based on optical absorption titrations of W191G with imidazole in 0.1 M BTP buffer, pH 6.0, as a function of $[K^+]$. Linear regression of the data to the equation $K_{obs} = K_d + (K_d/K_I)[K^+]$ gave the dissociation constant for the binding of imidazole to W191G in the absence of added K^+, $K_d = 0.11$ mM, and the dissociation constant for the binding of K^+ to W191G, $K_I = 18$ mM. The data point at 92 mM K^+ reported earlier (Fitzgerald et al., 1994) is shown as an open square. Inset: Representative Scatchard plots that show the competitive nature of K^+ and imidazole binding; ●, 49 mM K^+; ■, 33 mM K^+; ▲, 19 mM K^+; ▼, 9.5 mM K^+; ◆, 2 mM K^+.

ing to W191G (Fitzgerald et al., 1994). Thus, removal of the negative charge of Asp-235 appears to abolish entirely the binding of imidazoles to the protein.

Crystal structure analysis of the W191G–D235N double mutant confirms that the structure and dimensions of the W191G cavity are relatively unaffected by the additional D235N mutation (Fig. 2). Crystallographic data were collected to 2.1 Å resolution for crystals of W191G and W191G–D235N (Table 1). Each crystal was grown and maintained under identical conditions of cation concentration (40 mM K^+) at pH 6.0. As observed previously for W191G (Fitzgerald et al., 1994), the refined structure of W191G–D235N exhibits a well-defined cavity containing ordered solvent molecules in place of Trp-191, with little movement of the surrounding main-chain structure relative to the wild-type enzyme. Relative to the Asp-235 side chain in W191G, the carboxamide side chain of Asn-235 rotates ca. 26° about the C_α–C_β bond (χ_1). The most significant change in the protein structure relative to W191G is observed

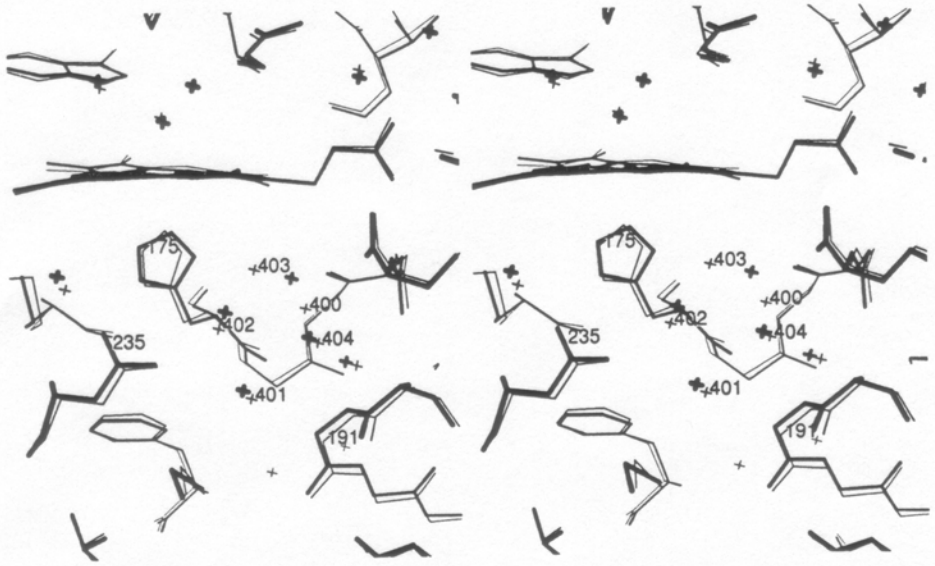

Fig. 2. X-ray crystal structures of the W191G and W191G–D235N mutants in 40 mM K^+, pH 6.0. Stereo views of the refined models for W191G (thin lines) and W191G–D235N (thick lines) at 2.1 Å resolution are superimposed, showing the relative positions of active-site residues and solvent molecules (labeled 400–404) in the vicinity of the cavity created by the Trp-191 to Gly mutation. Crystal structure determinations were performed for each mutant under the same conditions in 40 mM potassium phosphate buffer, pH 6.0, 28% MPD.

Table 1. *Data collection and refinement statistics*[a]

	W191G	W191G-D235N
Data collection		
Total reflections	60,429	48,753
Unique reflections	23,952	17,426
Unit cell[b]	Yeast	MKT
Resolution (Å)	2.1	2.1
$I/\sigma_{I(ave)}$	14.4	9.3
$I/\sigma_{I(last\ shell)}$	2.2	1.0
Completeness (%)	90	83
R_{sym}	0.047	0.074
Refinement		
R_{cryst}	0.168	0.195
Resolution (Å)	5.0-2.1	5.0-2.1
No. of reflections	20,827	15,258
RMS bond (Å)	0.013	0.015
RMS angle	2.6°	2.9°
No. of solvent molecules	97	53

[a] $R_{cryst} = \Sigma(F_{obs} - F_{calc})/\Sigma(F_{obs})$; $R_{sym} = \Sigma|I_h - \bar{I}_h|/\Sigma I_h$; RMS bond and RMS angle represent the RMS deviation between the observed and ideal values. Values of I/σ_I (last shell) represent that value for the 10% of the data of highest resolution.

[b] MKT and yeast refer to different crystal forms often seen with this enzyme having unit cell parameters (in Å) $a = 105.2$, $b = 74.3$, $c = 45.4$, and $a = 108.0$, $b = 77.3$, $c = 51.8$, respectively (Wang et al., 1990).

at the His-175 heme ligand, where the histidyl ring plane is rotated ca. 40° about the C_β-C_γ bond (χ_2). The structure of W191G-D235N is otherwise very similar to that of W191G.

Crystallographic analysis supports the observation that replacement of the Asp-235 carboxyl abolishes the imidazole binding properties of W191G. Shown in Figure 3A is an $F_{soaked} - F_{unsoaked}$ difference Fourier map contoured at $\pm 3\sigma$ for W191G crystals in the presence of 1 mM DMI, pH 6.0, or 40 mM potassium phosphate, pH 6.0. Significant difference features are observed, consistent with the displacement of solvent by DMI^+. No such difference density is evident in Figure 3B for the analogous experiment performed on crystals of W191G-D235N. Likewise, soaks of W191G-D235N crystals in 10 mM DMI ($pK_a = 7.9$) at pH 7.3 or 50 mM imidazole at pH 7.5 failed to show significant difference densities (data not shown). In these two experiments, significant concentrations of the neutral forms of the imidazoles are present. Thus, our crystallographic data are consistent with optical titrations that indicate that the W191G-D235N double mutant shows no observable imidazole or imidazolium binding behavior.

Significant changes are evident in the occupation of the solvent peaks within the cavity of W191G-D235N that indicate that removal of the carboxylate has modified the already weak potassium binding affinity. Fourier omit maps for the W191G-D235N double mutant indicated that the electron density peak, which we originally modeled as H_2O-400 in W191G (but which Miller et al. [1994] identified as a buffer cation), was observed at significantly reduced intensity and slightly shifted position for the W191G-D235N double mutant. In addition, the peak modeled as H_2O-403 in W191G is absent in W191G-D235N. To better characterize these observations, structures of W191G and W191G-D235N obtained in 40 mM K^+ were taken through several cycles of positional and *B*-factor refinement after all peaks within the cavity were modeled as water. For the W191G structure, the *B* value for H_2O-400 is 3.5 Å^2 (Table 2). This is significantly smaller than that observed for other waters in the cavity and represents the lowest *B* value for any water in the model. Our data are thus consistent with the assignment of this peak to a K^+ ion (Miller et al., 1994). However, the *B* value for the single peak replacing H_2O-400 and H_2O-403 (retaining the label H_2O-400) in W191G-D235N is 34.0 Å^2 (Table 2). This, together with the disappearance of H_2O-403, one of the potassium ligands in the interpretation of Miller et al. (1994), indicates at least a significantly diminished occupancy by K^+ in the double mutant. Other than Asp-235, all of the structural elements proposed to favor K^+ binding at this site, including the reverse turn of residues 174-177, the so-called "helix dipole" of residues 165-175, and the heme propionates (Miller et al., 1994), are retained in the W191G-D235N double mutant. It thus appears that the charged carboxylate of Asp-235 is important not only for imidazolium binding but for cation binding in general, and that the structural elements discussed by Miller et al. as the consensus K^+ site are not sufficient (but may still be necessary) for observable potassium binding.

Discussion

This study of the cavity created by the W191G mutant of CCP firmly establishes an important role for Asp-235 in the observed cation binding specificity. We previously reported that the electron density for imidazolium cations in the W191G cavity is consistent with an orientation enabling the proton on the unsubstituted nitrogen to interact with Asp-235 (Fitzgerald et al., 1994). This suggested that an ion-pair interaction may be important in stabilizing cationic species at this site. The present study shows that replacement of the carboxylate of Asp-235 with Asn abolishes all evidence for binding by imidazoles or potassium ions and thus fully supports earlier proposals (Goodin & McRee, 1993; Fitzgerald et al., 1994) that Asp-235 serves to significantly stabilize the Trp-191 cation radical.

In addition, this work serves to clarify two apparent differences in interpretation between the initial report of this cation binding cavity (Fitzgerald et al., 1994) and a subsequent study on a similar mutant (Miller et al., 1994). With regard to the identity of one of the five solvent electron density peaks within the "empty" cavity, our data are consistent with the interpretation

Table 2. *Refined B values for cavity peaks modeled as H_2O*

	B value (Å^2)	
Atom	W191G	W191G-D235N
H_2O-400	3.50	34.01
H_2O-401	16.44	32.12
H_2O-402	16.08	34.74
H_2O-403	21.15	Not observed
H_2O-404	25.07	38.94
All solvent molecules[a]	25.29	26.63
All heavy atoms[b]	19.13	22.54

[a] Average *B*-factor for all modeled water oxygens.

[b] Average *B*-factor for all nonsolvent heavy atoms.

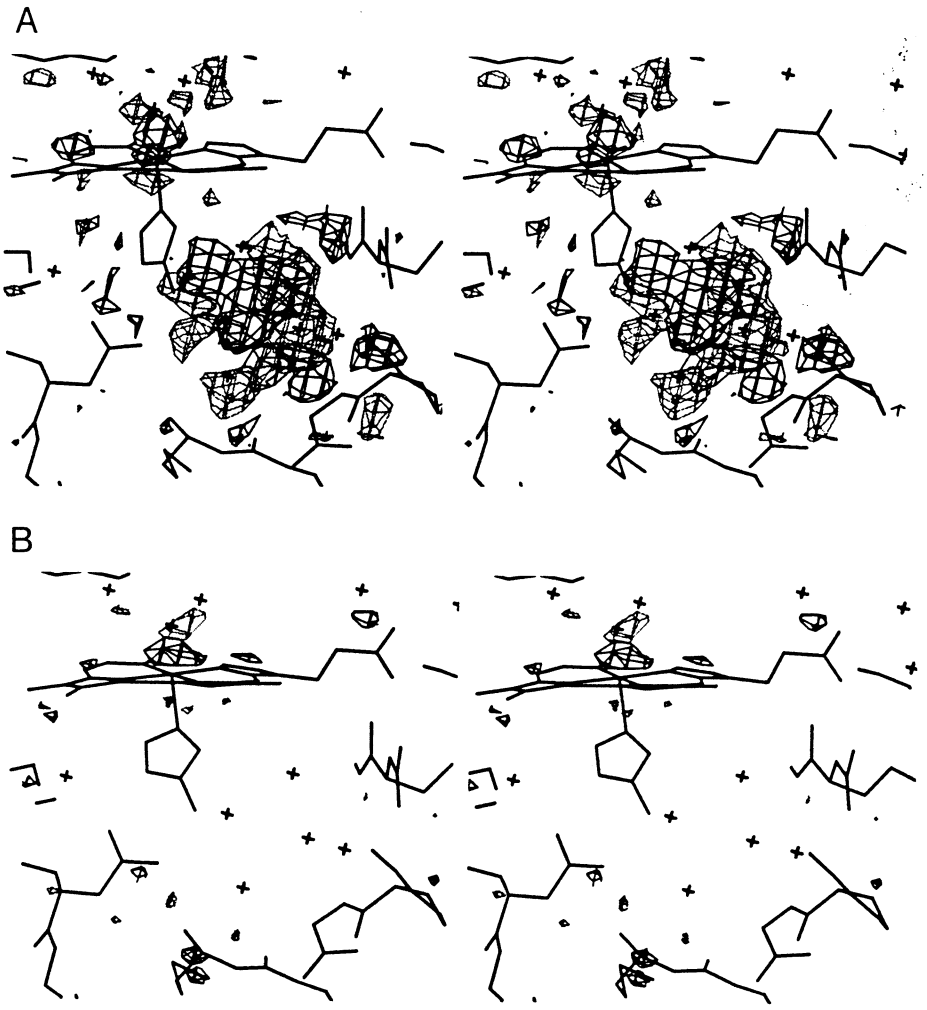

Fig. 3. Stereo views of ($F_{DMI} - F_{K^+}$) difference Fourier maps for (**A**) W191G and (**B**) W191G-D235N. Gray shading represents negative difference density contoured at -3σ; black shading represents positive difference density contoured at $+3\sigma$. Each map is superimposed on the appropriate refined model structure. Before data collection, crystals of W191G or W191G-D235N were soaked in 1 mM DMI, pH 6.0, in 28% MPD, or in 40 mM potassium phosphate, pH 6.0, in 28% MPD.

(Miller et al., 1994) that this feature results from binding of an alkali metal ion. Fourier difference features observed with different buffer cations (Miller et al., 1994) and the unusually low *B* value observed for a water molecule modeled at this site (Fitzgerald et al., 1994) prompted Miller et al. (1994) to suggest that this site was occupied by a buffer cation. Our current results, under defined conditions of potassium ion concentration, suggest that the *B* value previously obtained is indeed rather low to be assigned to a bound water. In addition, the binding studies presented clearly show the competitive nature of potassium and imidazole interactions with the cavity.

However, the relative significance that was assigned to the binding of cationic heterocycles versus buffer cations, which was derived from a number of assumptions about the relative binding affinities (Miller et al., 1994), is not supported by our data. The similarity of the potassium binding site, which is near the carbonyl oxygens of residues 175 and 177 of a Type III turn, to the cation binding sites of other structures led Miller et al. (1994) to assert that the cation binding site of W191G was not at the site of imidazole binding but rather at the potassium site. Although electrostatic calculations using a continuum dielectric model indicated a significant electrostatic stabilization of cationic species in the cavity, it was acknowledged that the choice of an appropriate macroscopic dielectric constant was problematic in quantitative evaluation of cation stabilization (Miller et al., 1994). Nevertheless, these calculations indicated that the stabilizing electrostatic field completely enveloped the W191G cavity, and contained significant contributions from Asp-235 as well as the main-chain carbonyls of residues 175 and 177, the heme propionates, and a "helix dipole." It is thus unclear why, in the absence of experimental data, the site of potassium binding was emphasized, whereas the importance of imidazole binding was dismissed. This study clarifies these assumptions by providing direct measurement of the relative affinities of these species and demonstrates that weak binding by K^+ to this cavity competes poorly with the much stronger binding by cationic imidazoles. Several factors may contribute to the higher affinities of imidazole compounds. The strength of the Asp-imidazolium ion pair may exceed that of the interaction of K^+ with its neutral ligands. The heterocyclic compounds may be able to distribute

charge over a greater area of the cavity as does the distributed spin density observed in the Trp-191 cation radical itself (Huyett et al., 1995). A larger contribution from the hydrophobic effect may also be expected for imidazole binding, as the more efficient filling of the cavity will affect the solvation energy. However, the complete loss of observed binding by charged or neutral imidazoles and the much lower occupation indicated at the potassium site in the W191G-D235N mutant suggest that entropic effects alone are not responsible for this difference in affinity and that the charge of Asp-235 is critical for both types of binding.

Further information about the role of electrostatic stabilization of the Trp-191 radical cation may arise from the recently reported structure of ascorbate peroxidase (APX) (Patterson & Poulos, 1995). The structure of this enzyme is very similar to CCP, and includes a proximal tryptophan (Trp-179) and the Asp-His-Trp environment that is observed in CCP. However, we have found that APX compound I does not contain a Trp radical intermediate (Patterson et al., 1995) but forms a porphyrin π-cation radical instead. A cation binding site located 8 Å from the relevant tryptophan (Trp-179) of APX is not observed in CCP and thus may play a role in destabilizing a cation radical at Trp-179 in APX (Patterson & Poulos, 1995; Patterson et al., 1995).

Taken together, all existing evidence appears to be in agreement that removal of the Trp-191 side chain leaves a buried cavity with an affinity for cations of a wide variety, and that different cations are uniquely stabilized by subsets of the interactions that stabilize the Trp-191 cation radical of the native enzyme. We predict that other cationic compounds would be stabilized by this cavity, and may do so by forming favorable interactions with each of the elements thus far identified. It is perhaps useful to consider that this cavity, as a whole, is much better at stabilizing imidazolium derivatives than alkali metal ions regardless of where within the cavity each species binds, because this may provide a more complete understanding of how the Trp-191 radical is stabilized by the enzyme.

Materials and methods

The W191G-D235N mutant of CCP-(MKT) was constructed by site-directed mutagenesis of the pT7CCP plasmid, overexpressed, and purified by methods described previously for the W191G mutant (Fitzgerald et al., 1994).

Competitive binding experiments were carried out by determining the observed dissociation constant, K_{obs}, for imidazole binding as a function of K^+ concentration. A 1 M stock solution of imidazole (Sigma) was adjusted to pH 6.0 with dilute H_3PO_4. W191G in potassium phosphate was exchanged into BTP buffer by passage through a Sephadex G-25 column equilibrated with 0.1 M BTP, pH 6.0. These potassium-free protein stock solutions were diluted in 0.1 M BTP, pH 6.0, to give an absorbance of 1.0 at the Soret maximum, and adjusted to the desired K^+ concentration using 1 M potassium phosphate buffer, pH 6.0. After equilibration at 24 °C for 30 min with stirring in a Hewlett-Packard 8452A diode-array spectrophotometer, the instrument was blanked, the solution was titrated with successive 1-μL additions of the appropriate dilution (0.1 M or 0.5 M) of the imidazole stock solution, and difference absorption spectra were taken after equilibration (~1 min). The observed dissociation constants, K_{obs}, for imidazole binding to W191G in the presence of K^+ were determined from Scatchard plots based on the difference absorbance at the wavelength of maximum difference and assumed one binding site per protein molecule. The K_I for K^+ was determined from the linear least-squares fit of the data to the equation $K_{obs} = K_d + (K_d/K_I)[K^+]$. We note that for the calculation of K_{obs} values, the total imidazole concentration, rather than the ionized imidazolium concentration, was used. At the pH of the measurements (pH 6), approximately 90% of the imidazole in solution is in the protonated state. Thus, the values obtained for K_d essentially represent the values for imidazolium rather than neutral imidazole binding (Fitzgerald et al., 1994) but are reported without correction for the equilibrium.

Single crystals of W191G or W191G-D235N for X-ray diffraction were grown by vapor diffusion from 25% MPD (Wang et al., 1990). Refined structures were obtained from one crystal of each mutant soaked for 1 h in 40 mM potassium phosphate pH 6.0 in 28% MPD. For experiments to examine imidazole binding, crystals of W191G or W191G-D235N were soaked at least 1 h in mother liquor containing 1 mM DMI adjusted to pH 6 with H_3PO_4 in 28% MPD to obtain F_{DMI}, and in 40 mM potassium phosphate, pH 6.0, in 28% MPD to obtain F_{K^+}. Cu K_α radiation from a Rigaku R-200 X-ray generator was used to measure X-ray diffraction data, which was collected at 15 °C with a Siemens X-1000 area detector. Data were processed with the XENGEN suite of programs (Howard et al., 1987). The XtalView package (McRee, 1992) was used to analyze data by difference Fourier techniques, and the program XPLOR (Brünger et al., 1987) was used for refinement.

Acknowledgments

This work was supported by funds from the National Institutes of Health (grants GM41049 to D.B.G., GM44841 and GM48495 to D.E.M., and GM15733 to M.M.F.). We are grateful to Prof. T.L. Poulos, Dr. Rabi Musah, Dr. Yi Cao, Sheri Wilcox, and Christopher Putnam for valuable discussions and critical comments.

References

Brünger AT, Kuriyan J, Karplus M. 1987. Crystallographic *R*-factor refinement by molecular dynamics. *Science 235*:458-460.

Dasgupta S, Rousseau DL, Anni H, Yonetani T. 1989. Structural characterization of cytochrome *c* peroxidase by resonance Raman scattering. *J Biol Chem 264*:654-662.

Erman JE, Vitello LB, Mauro JM, Kraut J. 1989. Detection of an oxyferryl porphyrin π-cation radical intermediate in the reaction between hydrogen peroxide and a mutant yeast cytochrome *c* peroxidase: Evidence for tryptophan-191 involvement in the radical site of compound I. *Biochemistry 28*:7992-7995.

Finzel BC, Poulos TL, Kraut J. 1984. Crystal structure of yeast cytochrome *c* peroxidase refined at 1.7 Å resolution. *J Biol Chem 259*:13027-13036.

Fishel LA, Farnum MF, Mauro JM, Miller MA, Kraut J, Liu YJ, Tan XL, Scholes CP. 1991. Compound-I radical in site-directed mutants of cytochrome-*c* peroxidase as probed by electron paramagnetic resonance and electron nuclear double resonance. *Biochemistry 30*:1986-1996.

Fitzgerald MM, Churchill MJ, McRee DE, Goodin DB. 1994. Small molecule binding to an artificially created cavity at the active site of cytochrome *c* peroxidase. *Biochemistry 33*:3807-3818.

Goodin DB, McRee DE. 1993. The Asp-His-Fe triad of cytochrome *c* peroxidase controls the reduction potential, electronic structure, and coupling of the tryptophan free radical to the heme. *Biochemistry 32*:3313-3324.

Houseman ALP, Doan PE, Goodin DB, Hoffman BM. 1993. Comprehensive explanation of the anomalous EPR spectra of wild-type and mutant cytochrome-*c* peroxidase compound-ES. *Biochemistry 32*:4430-4443.

Howard AJ, Gilliland GL, Finzel BC, Poulos TL, Ohlendorf DH, Salemme FR. 1987. The use of an imaging proportional counter in macromolecular crystallography. *J Appl Crystallogr 20*:383–387.

Huyett JE, Doan PE, Gurbiel R, Houseman ALP, Sivaraja M, Goodin DB, Hoffman BM. 1995. Compound ES of cytochrome c peroxidase contains a Trp π-Cation Radical: Characterization by CW and pulsed Q-band ENDOR. *J Am Chem Soc* (in press).

Katritzky AR, Rees CW. 1984. *Comprehensive heterocyclic chemistry, vol 4*. Oxford, UK: Pergamon Press.

McRee DE. 1992. A visual protein crystallographic software system for X11/Xview. *J Mol Graphics 10*:44–46.

McRee DE, Jensen GM, Fitzgerald MM, Siegel HA, Goodin DB. 1994. Construction of a bisaquo heme enzyme and binding by exogenous ligands. *Proc Natl Acad Sci USA 91*:12847–12851.

Miller MA, Han GW, Kraut J. 1994. A cation binding motif stabilizes the compound I radical of cytochrome *c* peroxidase. *Proc Natl Acad Sci USA 91*:11118–11122.

Patterson WR, Poulos TL. 1995. Crystal structure of recombinant pea cytosolic ascorbate peroxidase. *Biochemistry 34*:4331–4341.

Patterson WR, Poulos TL, Goodin DB. 1995. Identification of a porphyrin π-cation radical in ascorbate peroxidase compound I. *Biochemistry 34*:4342–4345.

Satterlee JD, Erman JE, Mauro JM, Kraut J. 1990. Comparative proton NMR analysis of wild-type cytochrome-*c* peroxidase from yeast, the recombinant enzyme from *Escherichia coli*, and an Asp-235 → Asn-235 mutant. *Biochemistry 29*:8797–8804.

Scholes CP, Liu Y, Fishel LA, Farnum MF, Mauro JM, Kraut J. 1989. Recent ENDOR and pulsed electron paramagnetic resonance studies of cytochrome *c* peroxidase-compound I and its site-directed mutants. *Isr J Chem 29*:85–92.

Sivaraja M, Goodin DB, Smith M, Hoffman BM. 1989. Identification by ENDOR of Trp 191 as the free-radical site in cytochrome *c* peroxidase compound ES. *Science 245*:738–740.

Spiro TG, Smulevich G, Su C. 1990. Probing protein structure and dynamics with resonance Raman spectroscopy: Cytochrome *c* peroxidase and hemoglobin. *Biochemistry 29*:4497–4508.

Vitello LB, Erman JE, Miller MA, Mauro JM, Kraut J. 1992. Effect of Asp-235 → Asn substitution on the absorption spectrum and hydrogen peroxide reactivity of cytochrome-*c* peroxidase. *Biochemistry 31*:11524–11535.

Wang JM, Mauro JM, Edwards SL, Oatley SJ, Fishel LA, Ashford VA, Xuong NH, Kraut J. 1990. X-ray structures of recombinant yeast cytochrome-*c* peroxidase and 3 heme-cleft mutants prepared by site-directed mutagenesis. *Biochemistry 29*:7160–7173.